

NUMERICAL MODELLING OF THE HYDROTHERMAL INFLUENCE OF THE GEOTHERMAL OPERATION WITH THE DCL SYSTEM IN THE EMBEDDING AQUIFERS: MULTI-PROBE CASE



Universidad de Oviedo



Hydro-Geophysics
and NDT Modelling Unit

July 2022

NUMERICAL MODELLING OF THE HYDROTHERMAL INFLUENCE OF THE GEOTHERMAL
OPERATION WITH THE DCL SYSTEM IN THE EMBEDDING AQUIFERS: MULTI-PROBE CASE

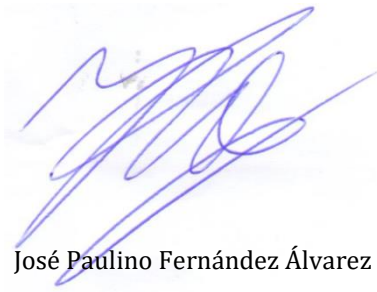
July-2022

Produced by:



Hydro-Geophysics
and NDT Modelling Unit
University of Oviedo

SCIENTIFIC DIRECTION



José Paulino Fernández Álvarez

*Mining engineer PHD
Coordinator of the Hydro-Geophysics and NDT Modelling Unit of the University of Oviedo*

TECHNICAL TEAM

Luis Calvo Buelga

*Civil engineer
Hydro-Geophysics and NDT Modelling Unit of the University of Oviedo*



TABLE OF CONTENTS

| | |
|--|----|
| 1. Introduction | 1 |
| 1.1. Problem statement..... | 1 |
| 1.2. Objectives | 1 |
| 2. Information and bibliography..... | 2 |
| 3. Numerical models | 4 |
| 3.1. Domain | 4 |
| 3.2. Initial heat condition (prior to pumping operation) | 5 |
| 3.3. Simulation scenarios | 6 |
| 3.4. Results..... | 7 |
| 4. Bibliography..... | 11 |
| Annex I: alternative study | 12 |

FIGURES

| | |
|---|---|
| FIG. 1-1. Operation diagram of the DCL® geothermal probe..... | 2 |
| FIG. 2-1.. A) Borehole with the differentiated lithology represented (DCL Geo-Energy) Data provided for the study. B) Surface temperature measurements in Alicante..... | 3 |
| FIG. 2-2. Flow and temperature scenarios. Probe operating times and temperatures (Itecon data). The flow of interest is fixed by the secondary flow. At the request of the company, a probe power of 90 kW is added to these data, with a secondary operating flow of 20 m ³ /h. | 3 |
| FIG. 3-1. Domain considered in the numerical modelling. (Left) 3D view of the domain of the model. (Right) Vertical section of the layered structure from the available lithological log (the 3 boreholes located in the central plane are observed). | 4 |
| FIG. 3-2. Hydraulic and thermal conditions for the case of study. Characteristics of the implemented mesh..... | 5 |

FIG. 3-3. Temperature distribution in depth. **(Left)** Stationary solution assuming a mean surface temperature. **(Right)** Depth temperature distributions for each month of the year. 6

FIG. 3-4. Evolution of the temperature at different depths of the model due to the seasonal variation of the surface temperature (1 year of simulation)..... 6

FIG. 3-5. Time evolution of the absolute temperature variation in the catchment **(left)** and injection **(right)** areas in the proposed scenarios. The time axis for the period of operation in summer is in the upper part of the graph ($t=0$ d is understood as the month of May), and for the winter period in the lower part ($t=0$ d corresponds to with the month of October). Note that the continuous, dashed, and dotted curves correspond to the position of the probes considered: central, side and corner, respectively..... 8

FIG. 3-6. Thermal influence at the catchment level in the proposed scenarios at the end of the geothermal operation ($t=150$ d) in the central evaluation plane. 9

FIG. 3-7. Visualization example of the results obtained from the numerical simulation. Isotherms of the system **(central evaluation plane)** after **150 days** of geothermal operation in the **winter season**, with an operating flow of **10 m³·h⁻¹**..... 9

FIG. 3-8. Visualization example of the results obtained from the numerical simulation. Isotherms of the System **(diagonal evaluation plane)** after **150 days** of geothermal operation in the **winter season**, with an operating flow of **10 m³·h⁻¹**..... 10

FIG. 3-9. Visualization example of the results obtained from the numerical simulation. Isotherms of the system **(central evaluation plane)** after **150 days** of geothermal operation in the **summer season**, with an operating flow of **10 m³·h⁻¹**..... 10

FIG. 0-1. Modification of the lithological characteristics of the medium. Water catchment and injection occur in the same aquifer. The distance between the injection and capture zones is increased. **(Left)** 3D view of the simulated domain. **(Right)** Vertical section of the layered structure considered (the 3 wells located in the central plane are observed)..... 12

FIG. 0-2. *Hydraulic and thermal conditions* 13

FIG. 0-3. Time evolution of the absolute temperature variation in the catchment area in the proposed scenarios. The time axis for the period of operation in summer is in the upper part of the graph ($t=0$ d is understood as the month of May), and for the winter period in the lower part ($t=0$ d corresponds to with the month of October). Note that the continuous,



dashed, and dotted curves correspond to the position of the probes considered: central, side and corner, respectively.....13

FIG. 0-4. Thermal influence at the catchment level in the proposed scenarios at the end of the geothermal operation ($t=150$ d) in the central evaluation plane.....14

FIG. 0-5. Visualization example of the results obtained from the numerical simulation. Isotherms of the system (**central evaluation plane**) after **150 days** of geothermal operation in the **winter season**, with an operating flow of $10 \text{ m}^3 \cdot \text{h}^{-1}$15

FIG. 0-6. Visualization example of the results obtained from the numerical simulation. Isotherms of the system (**central evaluation plane**) after **150 days** of geothermal operation in the **summer season**, with an operating flow of $10 \text{ m}^3 \cdot \text{h}^{-1}$15

TABLES

Table 1. Some ranges of hydrogeological and thermal properties of the study materials. .. 4

Table 2. Hydrogeological and thermal properties of study materials. **Average values used in the simulations**..... 4

Table 3. Sets of proposed simulation scenarios..... 7



1. INTRODUCTION

This project has been carried out by the **Hydro-Geophysics Modelling and Non-Destructive Testing Unit of the University of Oviedo** at the request of the Itecon company, interested in assessing the possible hydrothermal influence of the DCL system (with 9 probes in total) in surrounding aquifers through numerical simulation.

1.1. Problem statement

The R&D and innovation department of the Itecon company has developed a DCL® geothermal probe technology that integrates features of open loop systems and closed loop systems (both vertical and horizontal).

This geothermal system exchanges water with the aquifer in which it is located. Its operation consists in extraction of water at depth and its subsequent reinjection in a more superficial area, at the level of the water table of the aquifer.

As can be seen in Fig. 1-1, during the winter season water is collected at a certain temperature and, after having passed through the heat pump, it is reinjected at a lower temperature to the aquifer, since the heat from the collected water is used for indoor climatization.

On the other hand, the water reinjected into the aquifer during the summer season has a higher temperature than that at the extraction point, because in this case the goal is to cool the indoor installation.

In this study it is assumed –as part of the characteristic parameters of the system supplied by the company– that the difference between catchment and reinjection temperatures is constant and equal to 5°C.

The company is interested in knowing the influence of water reinjection process on the temperature of the fluid at the catchment area, both in the time and in its thermal magnitude, for a **system of 9 DCL probes** working together.

Once the problem has been exposed, the different objectives set in this project are listed.

1.2. Objectives

The main objective of the numerical modelling is to evaluate the effect of the extraction and reinjection of water on the surrounding aquifer.

For this goal, different scenarios considered of interest by Itecon are studied:

- Variation of temperature at any point in the domain over time, with special interest in the catchment and injection areas of geothermal probes.
- In the same way, the radius of thermal influence produced by the exchange of flow with the aquifer is estimated.

It is necessary to carry out a series of tasks:

- Conceptualization of the problem and construction of the geometric model.
- Choice of relevant factors in the study.
- Search for information related to the stratigraphic layers of the study location.
- Numerical simulation and results.

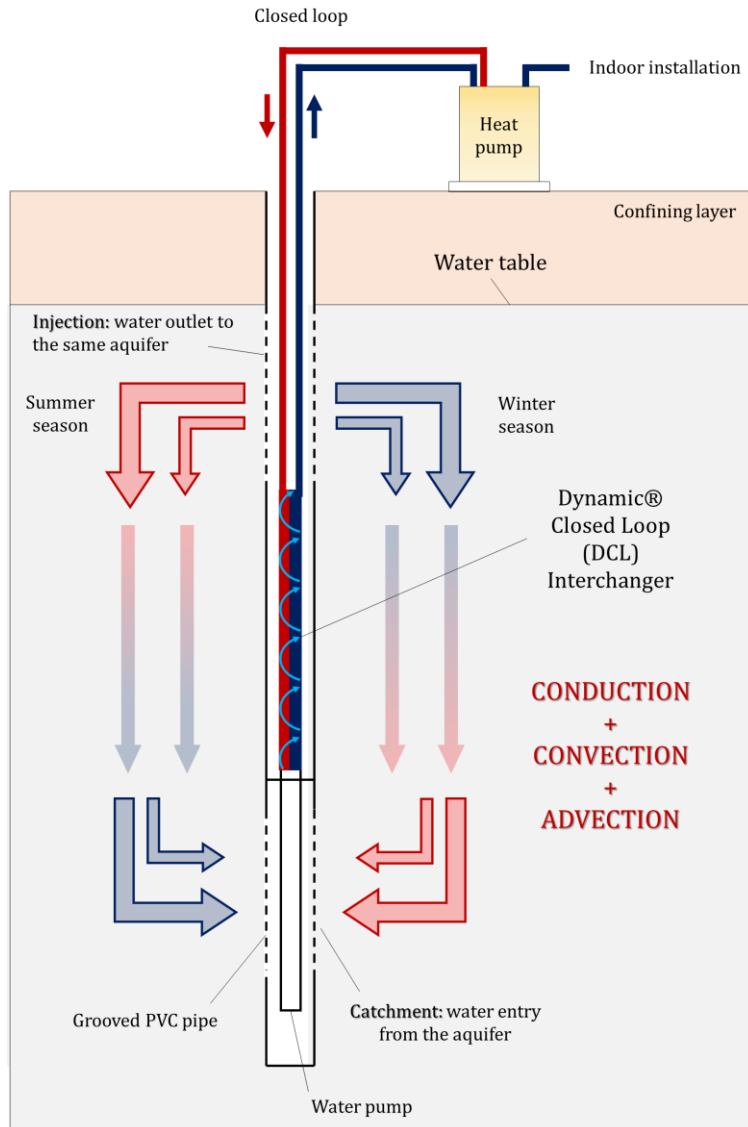


FIG. 1-1. Operation diagram of the DCL® geothermal probe

2. INFORMATION AND BIBLIOGRAPHY

The Itecon company has provided a basic documentation on which to develop the requested work:

- Analysis of the evolution and status of groundwater bodies used in times of drought in the Júcar Basin (*Hydrographic Confederation of Júcar and Geological and Mining Institute of Spain*, 2010).
- Highlights of the current hydrological year in the Valencian Community (*State Meteorological Agency*, 2017-2018).
- DCL Geo-Energy catalogue (Itecon).
- DCL Geothermal System, *Dynamic Closed Loop* (Itecon).
- Drilling scheme (Itecon). A series of 7 stratigraphic layers identified in the studied aquifer (Fig. 2-1).
- Excel file with flow and temperature scenarios (Itecon) (Fig. 2-2).
- Hydrogeological study of the *Parc Central*, Valencia (Itecon).

The agreed conditions for this study establish that it must be performed assuming both the stratigraphic and hydrodynamic properties of the materials that appear in the log as dominant throughout the aquifer. This can be seen in Fig. 2-1.

Layers are taken as homogeneous and isotropic. Regarding surface temperature, monthly average values in Alicante have been taken (see Fig.2-1).

Similarly, based on the data shown in Fig.2-2, different useful simulation scenarios for the company have been determined. Basically, they are differentiated by the time of year and the assumed operating flows (different installed pumping powers). The scenarios are detailed later in the document.

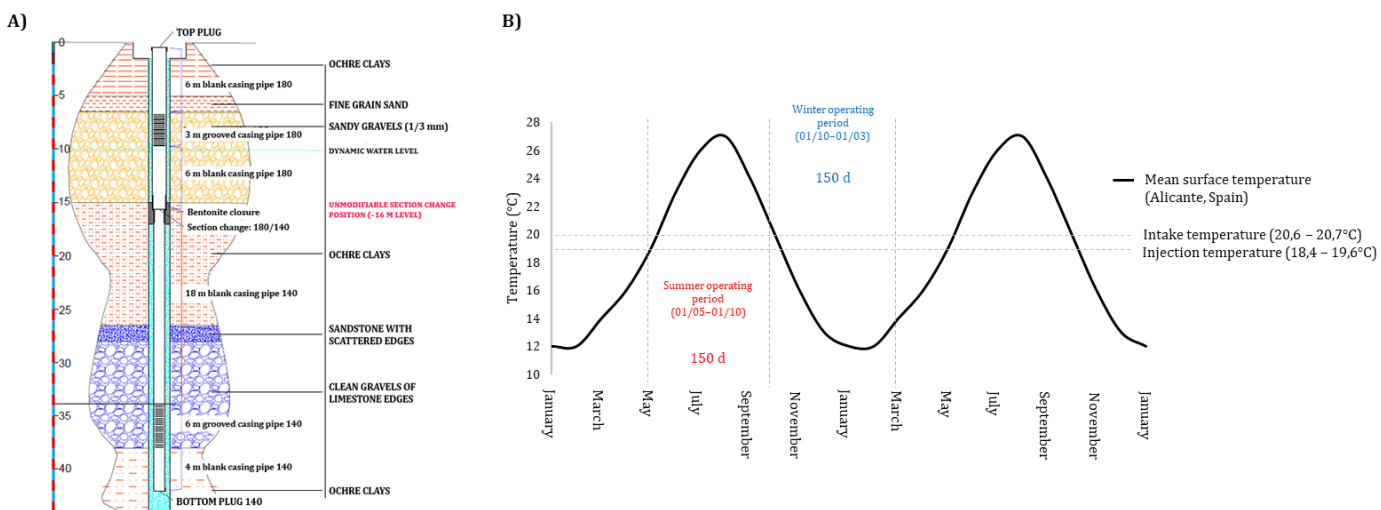


FIG. 2-1. A) Borehole with the differentiated lithology represented (DCL Geo-Energy) Data provided for the study. **B)** Surface temperature measurements in Alicante.

| PROBE POWER | Study temperatures and flow rates | | | | | | DAYS | H/DAY | KWH/DAY |
|-------------|-----------------------------------|--------------------------|---------------------------|------------------------------------|----------------------------|-----------------------------|------|-------|----------|
| | PRIMARY FLOW (m ³ /h) | PRIMARY INLET TEMP. (°C) | PRIMARY OUTLET TEMP. (°C) | SECONDARY FLOW (m ³ /h) | SECONDARY INLET TEMP. (°C) | SECONDARY OUTLET TEMP. (°C) | | | |
| 45 | 10 | 35 | 30 | 12 | 22 | 26.17 | 120 | 18 | 900.00 |
| | 10 | 32 | 28 | 12 | 24 | 27.33 | 150 | 18 | 720.00 |
| | 10 | 28 | 23 | 12 | 19 | 24.00 | 150 | 18 | 1,080.00 |
| 45 | 10 | 15 | 20 | 12 | 22 | 17.83 | 120 | 18 | 900.00 |
| | 10 | 13 | 17 | 12 | 18 | 14.67 | 150 | 18 | 720.00 |
| 70 | 15 | 35 | 30 | 18 | 22 | 26.17 | 120 | 18 | 1,350.00 |
| | 15 | 32 | 28 | 18 | 24 | 27.33 | 150 | 18 | 1,080.00 |
| | 15 | 28 | 23 | 18 | 19 | 24.00 | 150 | 18 | 1,620.00 |
| 70 | 15 | 15 | 20 | 18 | 22 | 17.83 | 120 | 18 | 1,350.00 |
| | 15 | 13 | 17 | 18 | 18 | 14.67 | 150 | 18 | 1,080.00 |

FIG. 2-2. Flow and temperature scenarios. Probe operating times and temperatures (Itecon data). The flow of interest is fixed by the secondary flow. At the request of the company, a probe power of 90 kW is added to these data, with a secondary operating flow of 20 m³/h.

To develop the required numerical models of groundwater flow and heat transport, it is necessary to indicate a series of parameters that define the hydrothermal behaviour of the aquifer to be studied, such as the density and porosity of the materials, their hydraulic and thermal conductivities, or their ability to store water and heat.

The Hydro-Geophysics and NDT Modelling Unit has an extensive database as a result of the updated comparison of different bibliographic sources. See, for example: [1, 2, 3, 4, 5] and, in the absence of local empirical information, possible ranges of values have been established for each material (table 1).

Table 1. Some ranges of hydrogeological and thermal properties of the study materials.

| MATERIAL | DENSITY (kg/m ³) | POROSITY (%) | HYDRAULIC CONDUCTIVITY (m/s) | STORATIVITY (m ⁻¹) | THERMAL CONDUCTIVITY (W/mK) | HEAT CAPACITY (J/kgK) |
|----------------------------------|------------------------------|--------------|------------------------------|---|-----------------------------|-----------------------|
| Sandy gravel 1/3 mm | 1400 – 2000 | 15 – 35 | 10^{-5} – 10^0 | 10^{-4} – $4.9 \cdot 10^{-5}$ | 1 – 2 | 900 – 1180 |
| Ochre clays | 1200 – 2680 | 0 – 2 | $< 10^{-7}$ | $2.6 \cdot 10^{-3}$ – $9.2 \cdot 10^{-4}$ | 1 – 2.9 | 860 – 920 |
| Sandstone with scattered edges | 2000 – 2600 | 0 – 20 | 10^{-10} – 10^{-4} | $< 3.3 \cdot 10^{-6}$ | 1.3 – 3.7 | 685 – 920 |
| Clean gravels of limestone edges | 1400 – 2000 | 15 – 35 | 10^{-5} – 10^0 | 10^{-4} – $4.9 \cdot 10^{-5}$ | 1 – 2 | 900 – 1180 |

A table of average values is also attached for guidance purposes (table 2).

Table 2. Hydrogeological and thermal properties of study materials. Average values used in the simulations.

| MATERIAL | DENSITY (kg/m ³) | POROSITY (%) | HYDRAULIC CONDUCTIVITY (m/s) | STORATIVITY (m ⁻¹) | THERMAL CONDUCTIVITY (W/mK) | HEAT CAPACITY (J/kgK) |
|----------------------------------|------------------------------|--------------|------------------------------|--------------------------------|-----------------------------|-----------------------|
| Sandy gravel 1/3 mm | 1700 | 25 | 10^{-3} | $5 \cdot 10^{-5}$ | 1.5 | 950 |
| Ochre clays | 2000 | 2 | 10^{-7} | 10^{-3} | 2 | 900 |
| Sandstone with scattered edges | 2300 | 10 | 10^{-5} | 10^{-6} | 2.5 | 900 |
| Clean gravels of limestone edges | 1700 | 25 | 10^{-3} | $5 \cdot 10^{-5}$ | 1.5 | 950 |

3. NUMERICAL MODELS

The numerical modelling presented in this section has been done with the simulation software *COMSOL Multiphysics®*.

3.1. Domain

The domain considered in the different numerical simulations is presented. In Fig.3-1 it is observed that it is a cylindrical 3D model with 9 boreholes located in its central area.

A vertically stratified (according to borehole in Fig. 2-1) and isotropic medium is considered. The layers of material are assumed horizontal in all their extension.

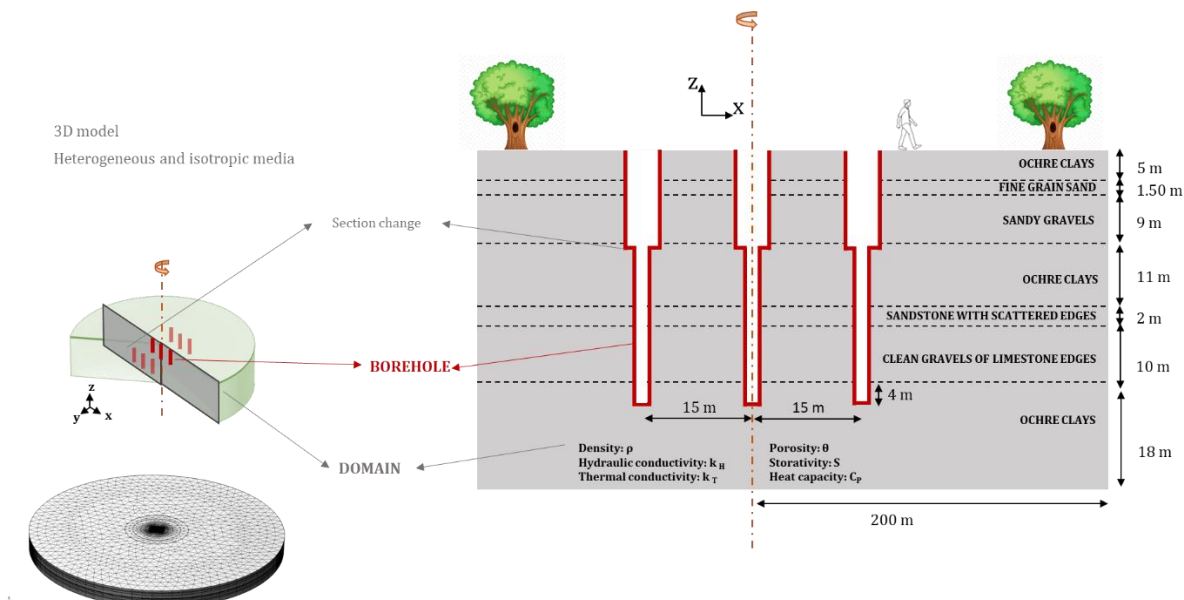


FIG. 3-1. Domain considered in the numerical modelling. (Left) 3D view of the domain of the model. (Right) Vertical section of the layered structure from the available lithological log (the 3 boreholes located in the central plane are observed).

The domain considered is set at 400 m radius and more than 50 m depth. These distances are enough to prevent the numerical limits of the domain to have any impact on the simulation.

In Fig. 3-2 the water catchment and injection areas can be distinguished in blue (6 and 3 m slotted sections). The radius of the well decreases with depth (90 mm at the top, 70 mm at the bottom). However, this variation in the radius of the survey involves significant meshing and computational problems, while its impact on the simulation results is negligible. Therefore, it is decided to assume the uniform borehole section and use a radius of 100 mm.

In the same figure it can be seen how the catchment and injection flows are the same, while the injection temperature depends directly on the water temperature in the catchment area at each moment of the operation process. In the winter operating period, the injection temperature is 5°C lower than that of the captured water, while in the summer operating period it is 5°C higher. The position of the water table is at the injection level (-6.50 m).

Finally, the natural geothermal heat flux considered in the study area is 80 mW·m⁻², based on the bibliography consulted [13], and together with the surface temperature, is used to calculate the initial temperature condition of the study system.

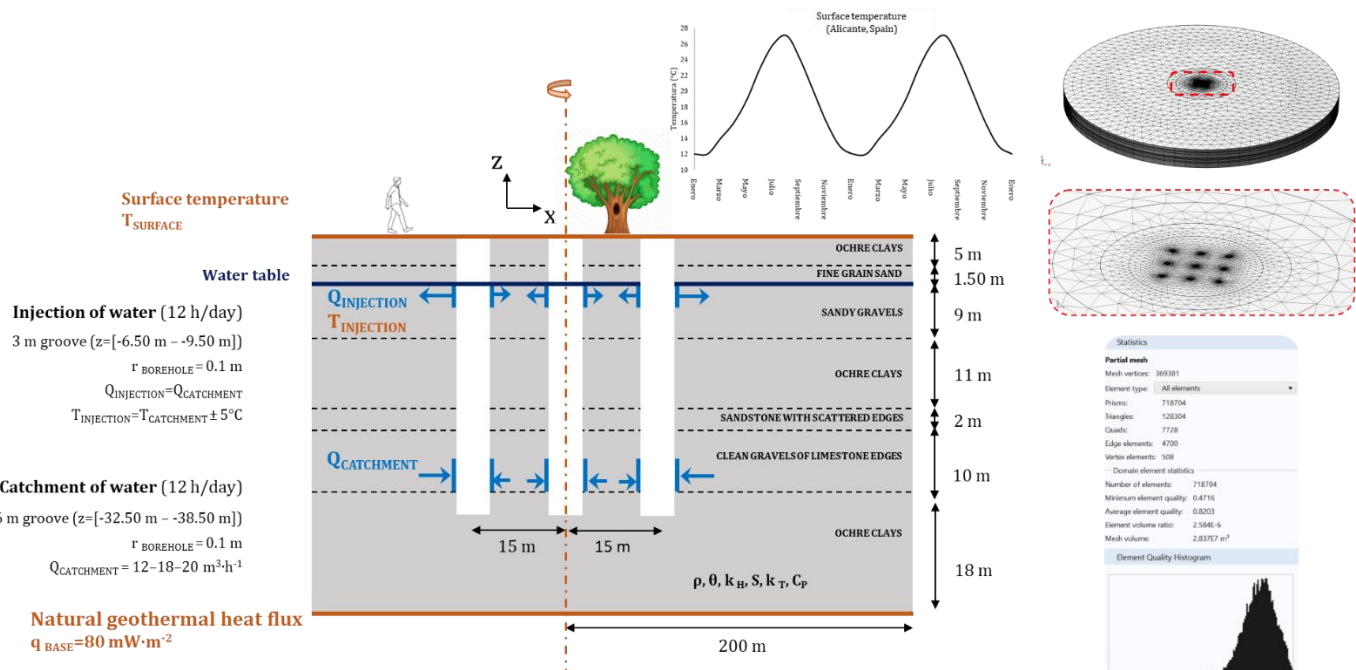


FIG. 3-2. Hydraulic and thermal conditions for the case of study. Characteristics of the implemented mesh.

3.2. Initial heat condition (prior to pumping operation)

The initial heat condition of the model is conditioned by two factors:

- Seasonal variation of the surface temperature of the model.
- Natural geothermal heat flux in the study area.

The subsurface temperature distribution *at the start* of the two operational periods specified must be calculated. The results are shown in Fig. 3-3 and are to be used as initial heat conditions in later models.

The average annual temperature in Alicante ($T_{MEAN}=19^{\circ}\text{C}$), the average monthly temperature of Alicante (graph Fig.2-1 and Fig.3-2) and the natural heat flux of the area ($80 \text{ mW}\cdot\text{m}^{-2}$) have been employed.

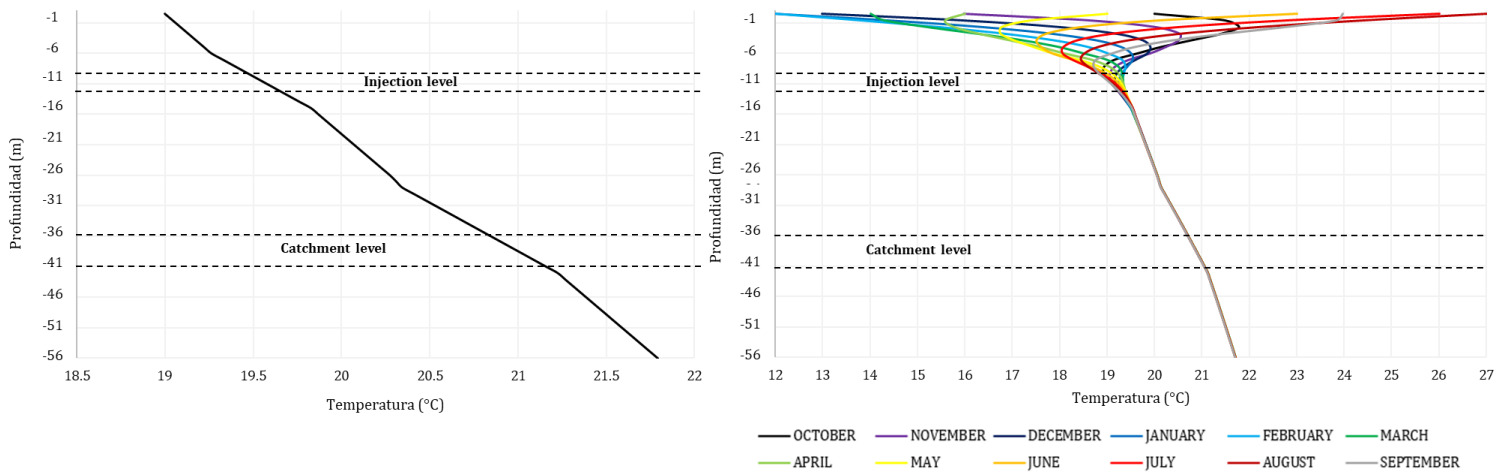


FIG. 3-3. Temperature distribution in depth. **(Left)** Stationary solution assuming a mean surface temperature. **(Right)** Depth temperature distributions for each month of the year.

Based on the results obtained, the temperatures at different depths are plotted over a 1 year of simulation (surface, catchment, and injection areas, see Fig. 3-4).

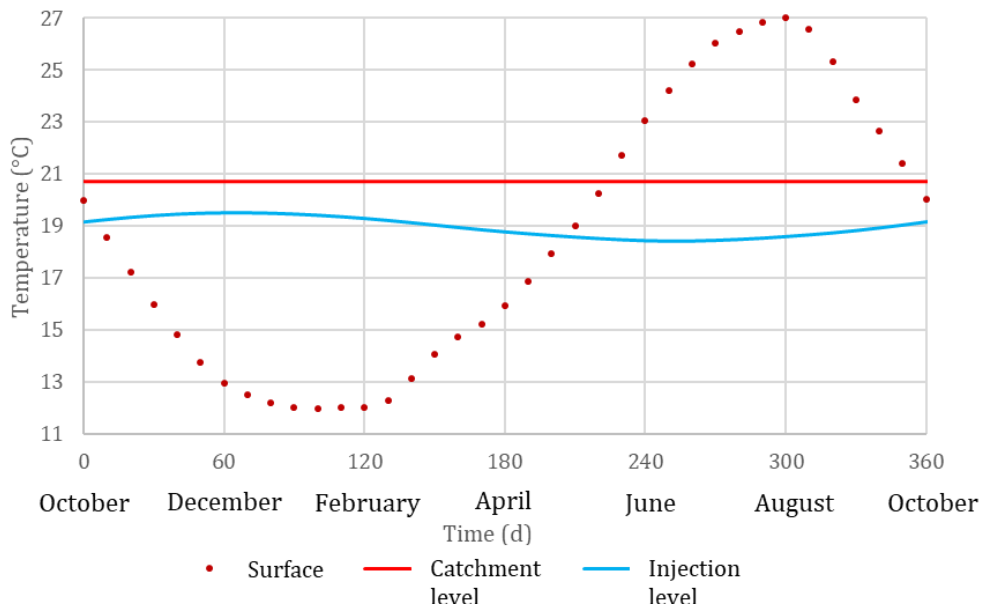


FIG. 3-4. Evolution of the temperature at different depths of the model due to the seasonal variation of the surface temperature (1 year of simulation).

The temperature at the injection depth (evaluated at -8 m [-6.50 – -9.50 m]) is only a little influenced by the seasonal variation of the surface temperature and oscillates between 18.4°C and 19.6°C prior to any type of geothermal operation.

The temperature at the catchment depth (evaluated at -35.50 m [-32.50 – -38.50 m]) does not almost change throughout the simulation, it remains stable at 20.65°C (within the range of real temperatures measured at the catchment elevation, Fig.2-2).

3.3. Simulation scenarios

From the data provided relative to the geothermal operation of the DCL probe at the study area in Alicante, some useful simulation scenarios have been determined for the study.

In the first place, two scenarios are clearly differentiated according to the time of year in which the operation takes place, whether it is the **winter operating period** (autumn-winter,

the temperature of the injected water is 5°C lower than that of the collected water) or *the summer operating period* (spring-summer, the injection temperature is 5°C higher than the catchment temperature in depth).

The geothermal operation of the DCL system, as agreed with the company, is considered to work for 12 hours a day and to be at rest the remaining 12 hours. As a simplified way to take this into account –proven to have no impact in the numerical results– is to simulate a continuous 24-hour operation of the pump with only half provided flow. For simulation purposes, flow rates of 6, 9 and 10 m³·h⁻¹ are adopted (instead of 12, 18 and 20 m³·h⁻¹, Fig.3-2) for each scenario proposed (table 3).

According to the initial operation data (Fig.2-2), the geothermal operation times are 120 and 150 days (both in the summer and in the winter period). Therefore, both operations will be simulated at 120 and 150 days.

Thus, table 3 shows the scenarios according to the two parameters considered: geothermal operation season (winter or summer) and the time in which the predictions are required. For all the scenarios, the 3 possible operating flows are considered.

Table 3. Sets of proposed simulation scenarios.

| SCENARIO | OPERATING PERIOD | T _{INJECTION} (°C) | t _{OPERATION} (d) |
|----------|------------------|-----------------------------|----------------------------|
| 1 | Summer period | + 5 | 150 |
| 2 | | | 120 |
| 3 | Winter period | - 5 | 150 |
| 4 | | | 120 |

3.4. Results

This section shows the results obtained by numerical simulations with the proposed scenarios. In view of the objectives set, two types of graphs are shown:

- Variation of catchment and injection temperatures over time *with respect to the existing temperatures, at that same point, in the absence of geothermal operation* (Fig. 3-5).
- Radii of the thermal influence at the catchment level at the end of each probe operation period. This radius is taken as the measured distance from the well at which the temperature varies only 0.1°C with respect to the assumption of no geothermal operation (Fig. 3-6).

Furthermore, domain isotherm visualizations are included for some of the simulated scenarios of interest (Fig. 3-7, Fig.3-8 and Fig.3-9).

In Fig. 3-5 it can be seen how in both *winter and summer operating periods* the catchment temperature barely varies (less than 0.25°C of variation).

Regarding the variation of the injection temperature, the different thermal jump at winter and summer scenarios deserves some explanation. In the summer operating period, a jump of 6.5°C is observed. In the winter operating period, the jump is, instead, - 4°C. This is because the re-injection, performed at points in the depth range between - 6.50 m and - 9.50 m, is influenced by the surface temperature in different magnitude depending on the season.

We must remind that the graphs represent the change in temperature at a point, *with reference to* the temperature at the same point *before* the operation of the system. Implied is also, therefore, that before the operating period, the system was operationally at rest. Only natural conditions were present. This is important if continuous operation for more

than one operating period is intended, as the adequate reference temperature for one period depends upon the final temperatures of the previous operating period. This would require more in-depth numerical simulation and would pertain rather to an activity seeking the optimal operational sequence, not dealt with in this report.

Having said all this, in the month of October, the initial (before operation) temperature at the re-injection depth is 1°C higher than the catchment temperature and therefore, cooling the catchment water by 5°C from operation principles means lowering 4°C the temperature at the re-injection depth in the winter period.

On the other hand, in May, the injection temperature is, under natural conditions before the pump operation starts, already 1.5°C lower than the catchment temperature. So, when the pump adds 5°C to the catchment temperature, the water acquires a temperature 6.5°C *higher* than the initial temperature at the injection point in the summer period.

The results of Fig.3-5 differentiate the three types of probes that are evaluated in these simulations and that present different behaviours among themselves (1 central probe, 4 side probes and 4 corner probes). On the other hand, in Fig.3-6, 3 evaluation planes are considered (central plane, side plane and diagonal plane).

With the accepted lithology and for the operating conditions studied, the catchment temperature can be considered constant during geothermal exploitation (maximum variation of the intake temperature of 0.25°C, Fig.3-5).

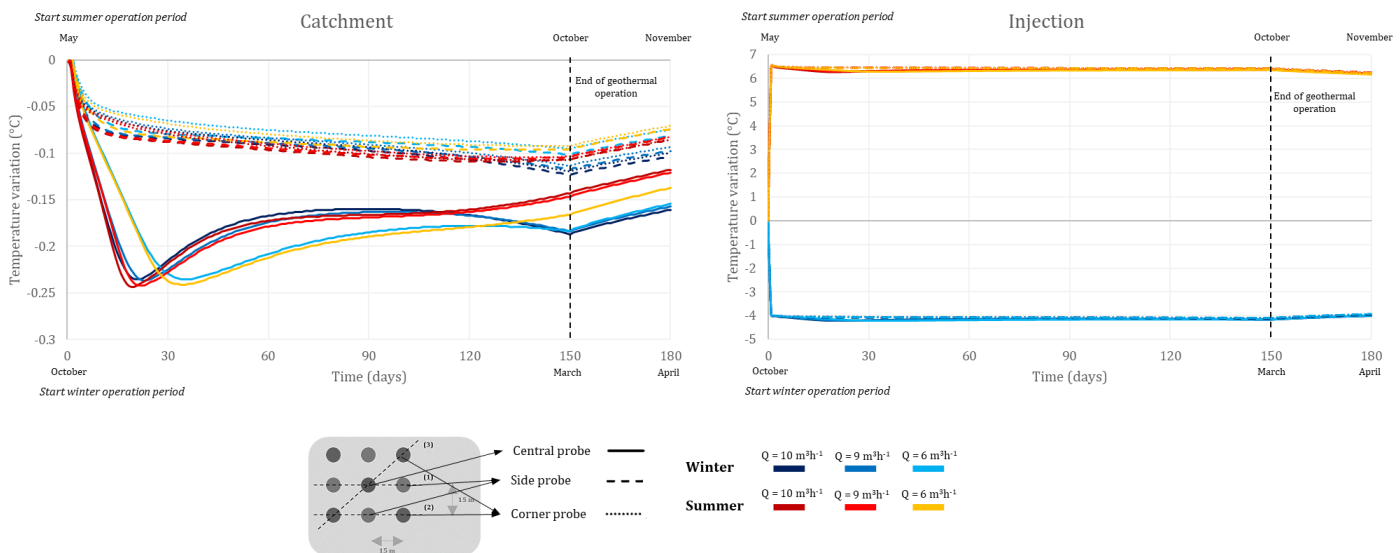


FIG. 3-5. Time evolution of the absolute temperature variation in the catchment (left) and injection (right) areas in the proposed scenarios. The time axis for the period of operation in summer is in the upper part of the graph ($t=0$ d is understood as the month of May), and for the winter period in the lower part ($t=0$ d corresponds to the month of October). Note that the continuous, dashed, and dotted curves correspond to the position of the probes considered: central, side and corner, respectively.

Regarding the radii of thermal influence on the catchment level, in Fig.3-6 it can be seen how, at the end of the geothermal operation (after 150 days), the temperature barely varies 0.2°C in the central zone of the model (location of the probes) and around 0.1°C in the rest of the domain. As with the previous graph, it can be concluded that the catchment temperature is not affected by the injection temperature and remains constant during the simulation. The radius of influence in the catchment area is approximately 20 m for the winter and summer scenarios with maximum flow.

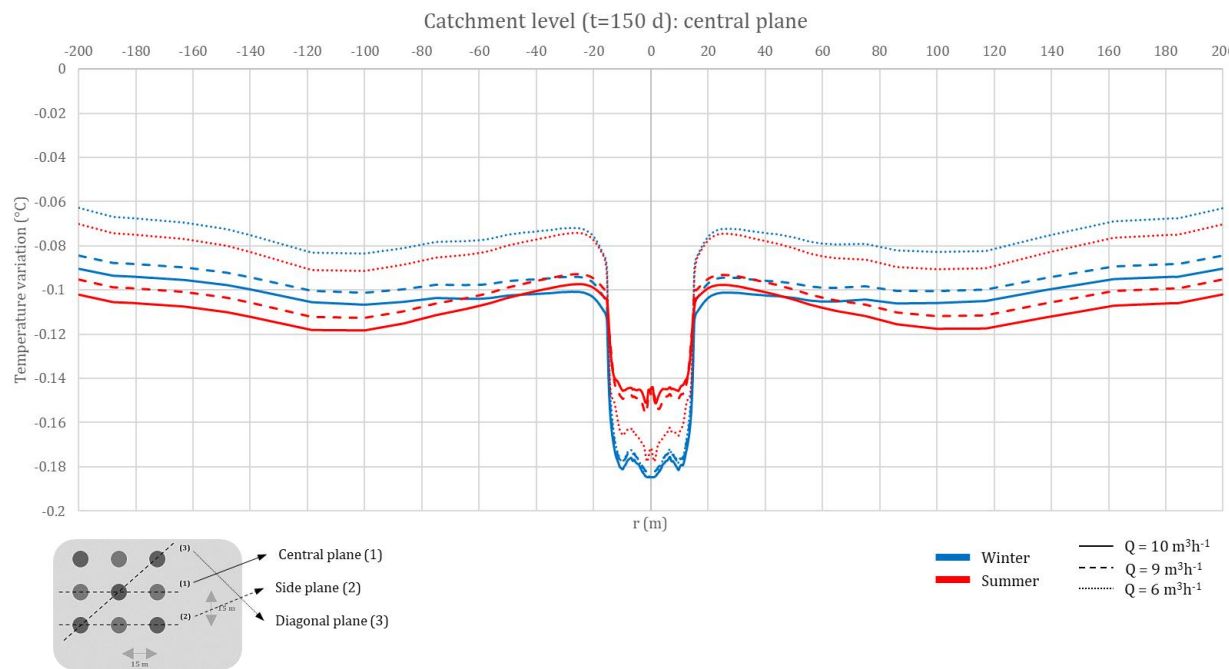


FIG. 3-6. Thermal influence at the catchment level in the proposed scenarios at the end of the geothermal operation ($t=150$ d) in the central evaluation plane.

Finally, Figs. 3-7, 3-8 and 3-9 show the isotherms in different evaluation planes (central and diagonal) resulting from the simulation of different scenarios (winter and summer seasons), with an operation flow rate of $10 \text{ m}^3/\text{h}$, at the end of the geothermal operation ($t=150$ d).

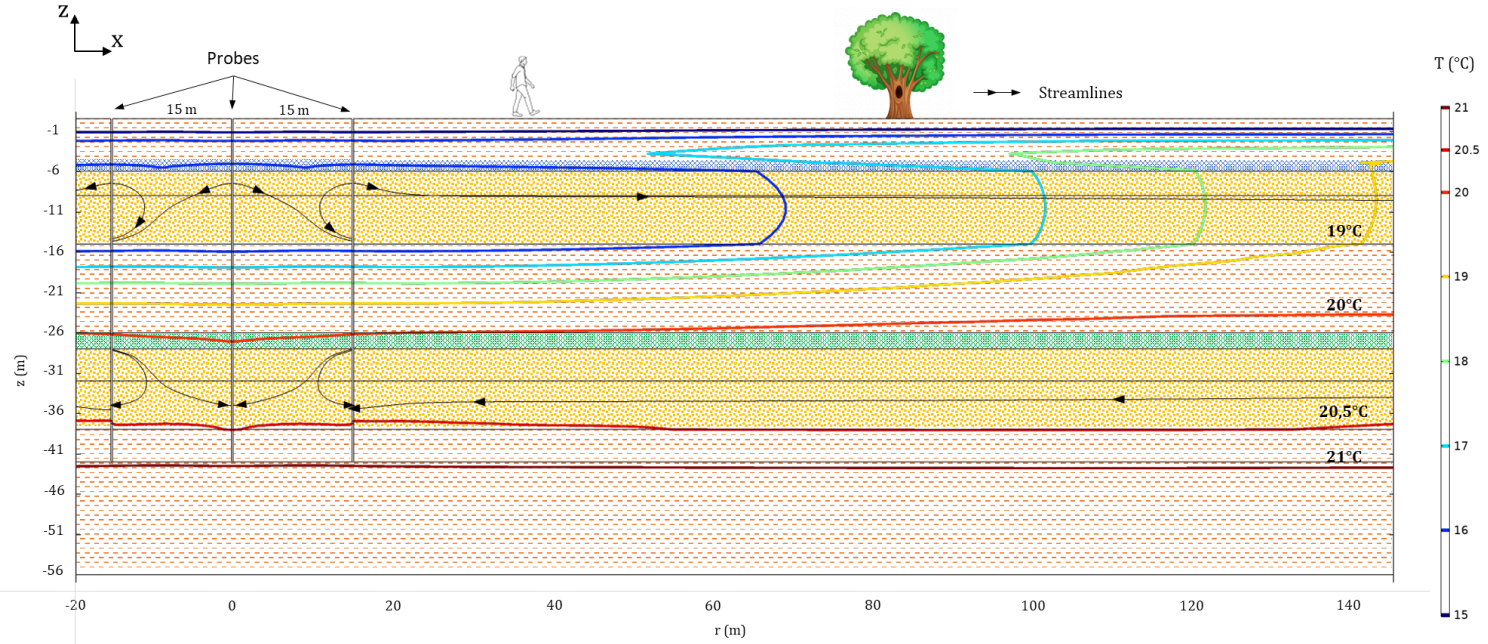


FIG. 3-7. Visualization example of the results obtained from the numerical simulation. Isotherms of the system (central evaluation plane) after 150 days of geothermal operation in the winter season, with an operating flow of $10 \text{ m}^3 \cdot \text{h}^{-1}$.

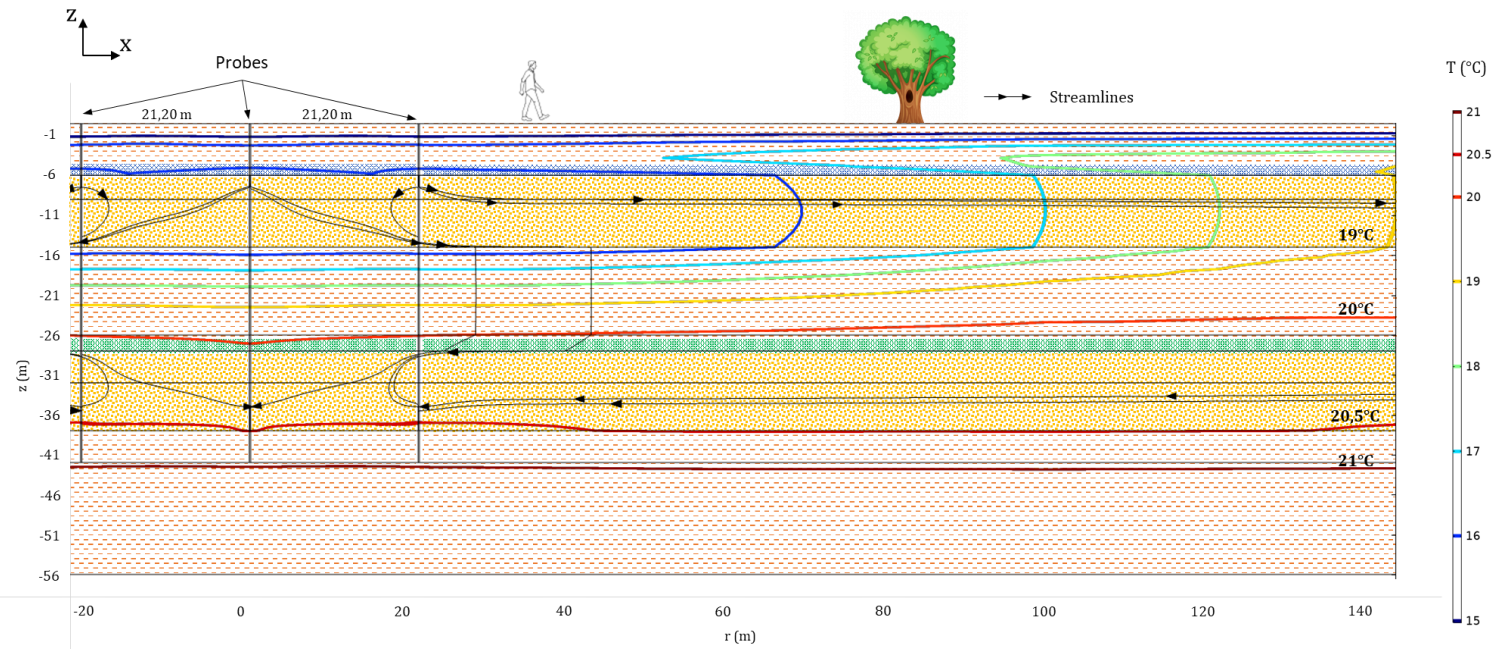


FIG. 3-8. Visualization example of the results obtained from the numerical simulation. Isotherms of the System (diagonal evaluation plane) after 150 days of geothermal operation in the **winter season**, with an operating flow of $10 \text{ m}^3 \cdot \text{h}^{-1}$.

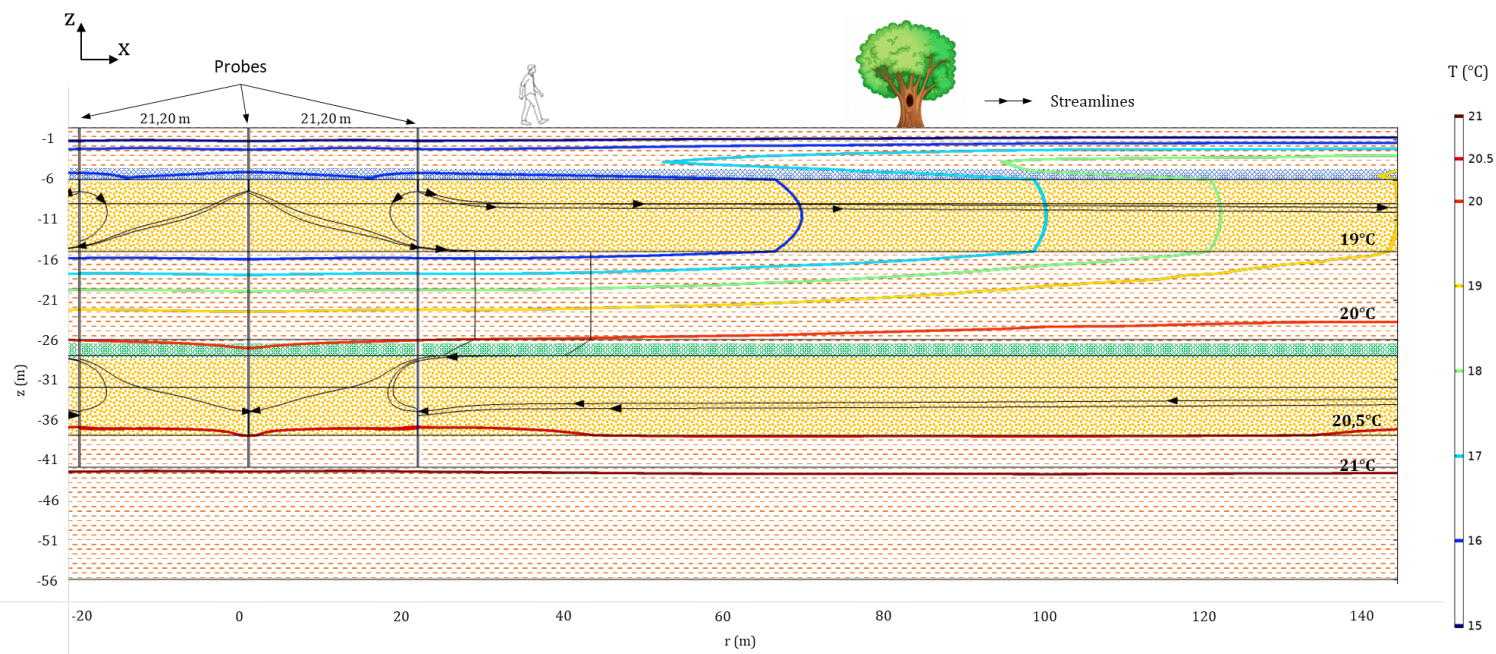


FIG. 3-9. Visualization example of the results obtained from the numerical simulation. Isotherms of the system (central evaluation plane) after 150 days of geothermal operation in the **summer season**, with an operating flow of $10 \text{ m}^3 \cdot \text{h}^{-1}$.



4. BIBLIOGRAPHY

- [1] Domenico, P.A. et.al (1998). *Physical and chemical hydrogeology*. Wiley, 508 pp.
- [2] Fetter, C.W. (2001). *Applied Hydrogeology*. Prentice-Hall, 4^a ed., 598 pp.
- [3] Sanders, L. (1998). *A manual of Field Hydrogeology*. Prentice-Hall, 381 pp.
- [4] Smith, L. et.al (1993). *Groundwater Flow*. In: Maidment, D.R. (Ed.). *Handbook of Hydrology*. McGraw Gill.
- [5] Beardsmore & Cull (2001). *Crustal Heat Flow. A guide to measurement and modelling*. (Cambridge University Press).
- [6] COMSOL Multiphysics, *Reference Guide*, Versión 4.3a, (n.d.).
- [7] J. Sánchez San Román (2014). *Ley de Darcy. Conductividad hidráulica*, Univ. Salamanca (España), Dep. Geol. (2014) 1-13. <http://diarium.usal.es/javisan/hidro>.
- [8] J. Werner, *Introducción a Hidrogeología*, 1st ed., 1996
- [9] F. de J.A. Vargas, *Modelación y simulación hidrodinámica del sistema acuífero Zamora*, en Michoacán México, (2010).
- [10] L. Smith, J. Weathcraft (1993). *Groundwater Flow*, in: Handb. Hydrol., In E. McGr.
- [11] M. P. Anderson, W. W. Woessner & R. Hunt (2015). *Applied groundwater modeling: simulation of flow and advective transport*. Academic Press Inc., San Diego.
- [12] Bundschuh, J., Suárez, M. (2010). *Introduction to the Numerical Modeling of Groundwater and Geothermal Systems*.
- [13] Albert J.F. (1979). *El mapa de flujos caloríficos. Intento de correlación entre anomalías geotérmicas y estructura cortical*. Boletín Geológico y Minero, T.XC-I (Energía), 36-48.
- [14] Xianzhi Song et.al (2019). *Numerical analysis on thermal characteristics of an open loop geothermal system in a single well*. Energy Procedia 158 (2019) 6112-6117. 10th International conference on applied energy (ICAE2018), 22-25 August 2018, Hong Kong, China.
- [15] Gaosheng Wang et.al (2019). *Numerical investigation on heat extraction performance of an open loop geothermal system in a single well*. Geothermics 80 (2019) 170-184. doi.org/10.1016/j.geothermics.2019.03.005.

Fdo: José Paulino Fernández Álvarez

ANNEX I: COMPLEMENTARY STUDY

As a complementary study to the one presented in this document, a new case is proposed in which the lithological characteristics of the aquifer, where the set of 9 DCL probes are installed, are modified.

The difference with respect to the materials presented in Figs.2-1, 3-1 and 3-2 consists in substituting the intermediate materials between the catchment and the injection **by a homogeneous aquifer of sandy gravel** (see *sandy gravel* parameters considered in table 2), limited in its base and in its surface by layers of clay (Figs.0-1 and 0-2).

As keeping the intake point at the same depth will produce a noticeable thermal impact there, the question analysed here is how much the distance between the injection and catchment areas must be increased, to allow normal operation of the probe.

The numerical results show that, taking the catchment point at practically the double depth (62 m) than the previous case (Fig.2-1, 32 m in total: 9m+11m+2m+10m) will suffice.

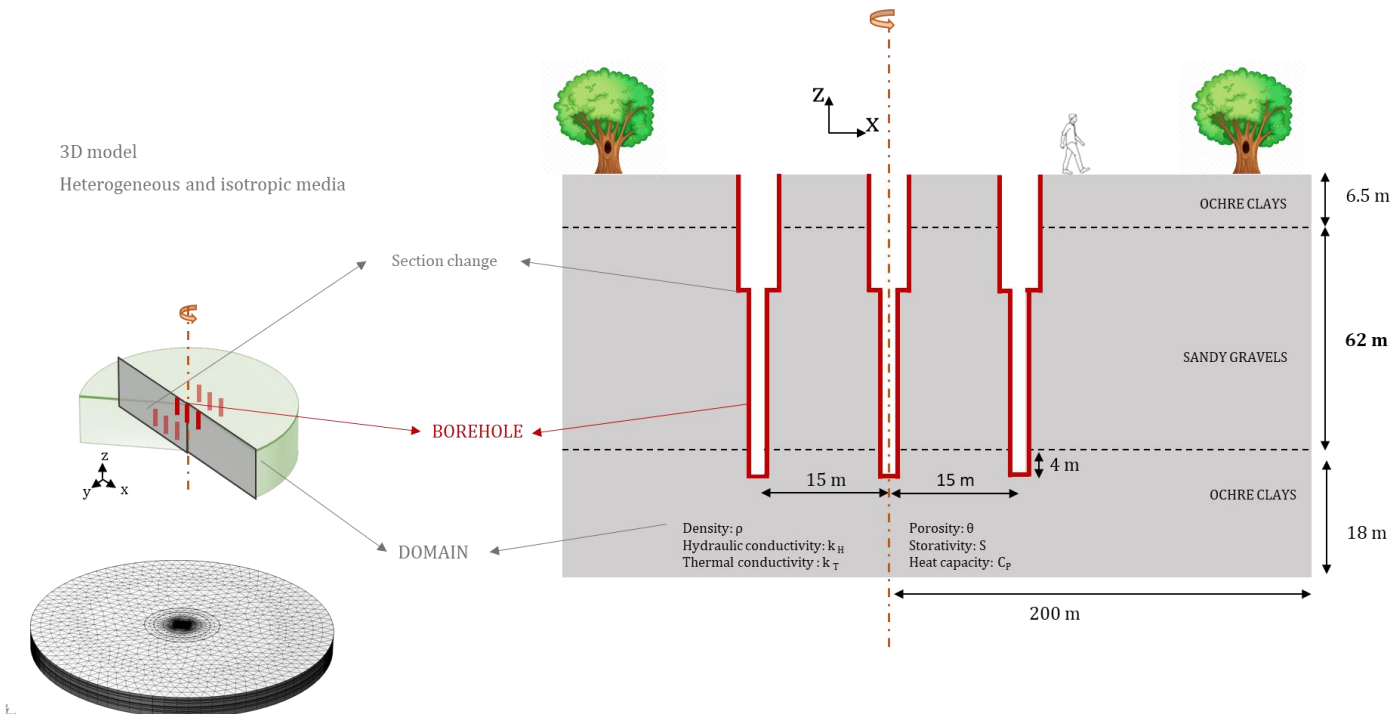


FIG. 0-1. Modification of the lithological characteristics of the medium. Water catchment and injection occur in the same aquifer. The distance between the injection and capture zones is increased. (Left) 3D view of the simulated domain. (Right) Vertical section of the layered structure considered (the 3 wells located in the central plane are observed).

To carry out this study, the initial conditions have been calculated again with the new material distribution, therefore, the temperature profiles in depth prior to any geothermal operation is also slightly modified from that shown in Fig.3-3.

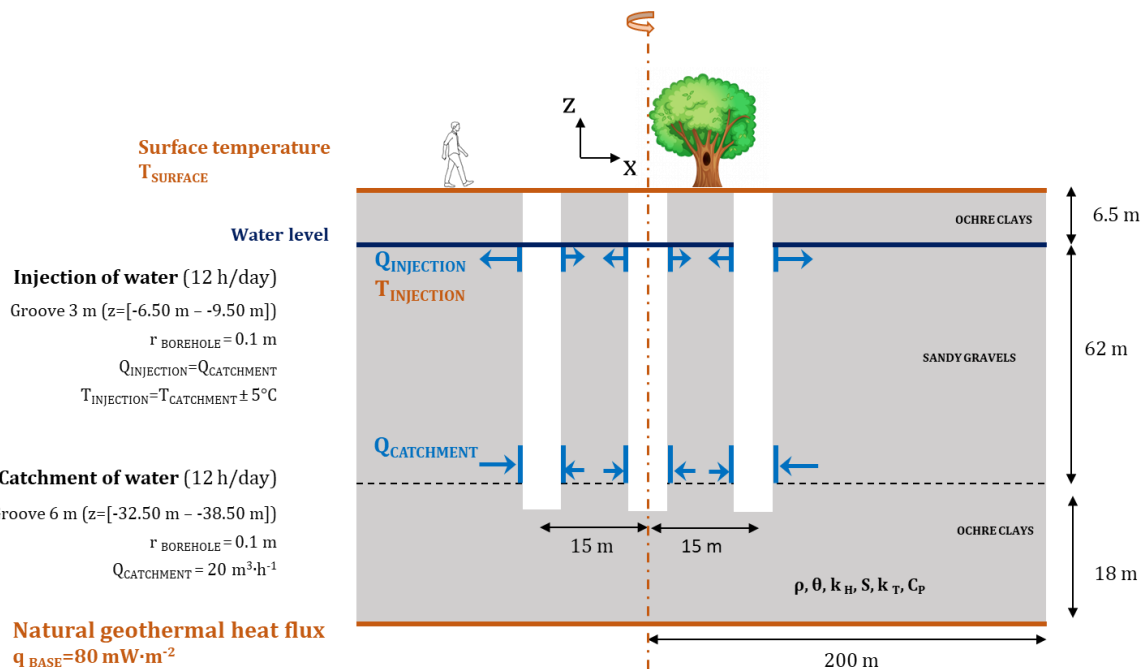


FIG. 0-2. Hydraulic and thermal conditions.

The temperature variations in the three types of probes considered (central, side and corner) throughout the 150 days of geothermal operation, both in winter and in summer seasons, for the case with the **highest operating flow rate** (10 m³/h for 24 h/day), can be observed in Fig.0-3.

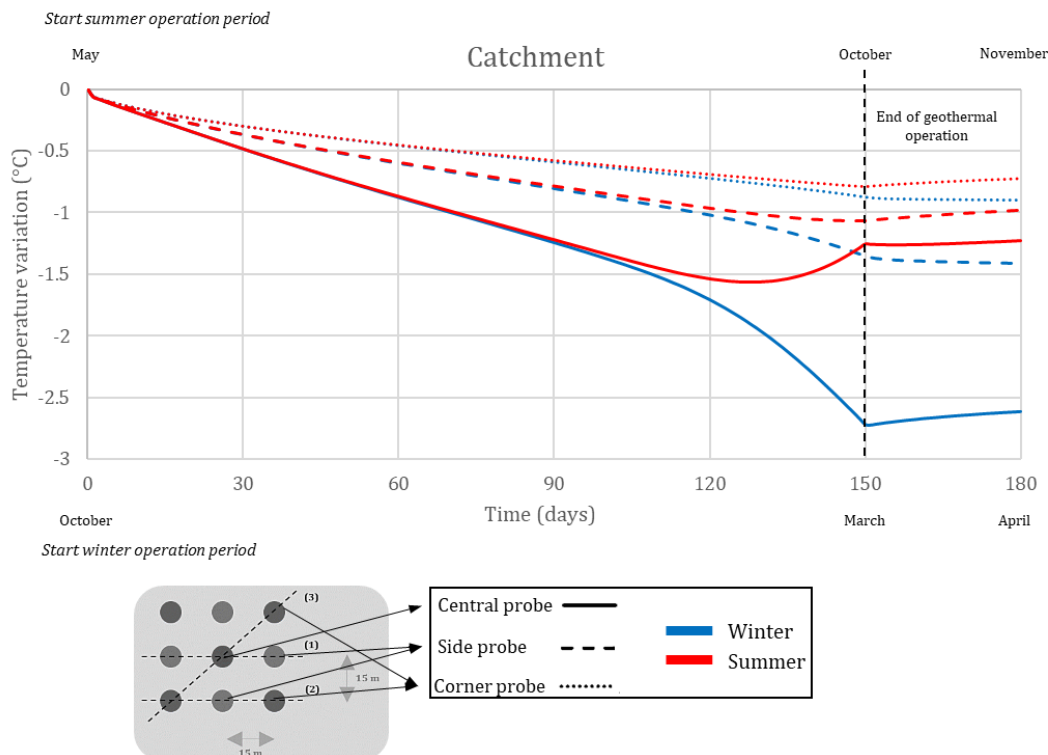


FIG. 0-3. Time evolution of the absolute temperature variation in the catchment area in the proposed scenarios. The time axis for the period of operation in summer is in the upper part of the graph ($t=0 \text{ d}$ is understood as the month of May), and for the winter period in the lower part ($t=0 \text{ d}$ corresponds to the month of October). Note that the continuous, dashed, and dotted curves correspond to the position of the probes considered: central, side and corner, respectively.

The results shown in the previous graph show how in winter periods, the intake temperature (central probe, continuous line) decreases by a maximum of 2.7°C , while in summer it decreases by a maximum of 1.6°C .

Both in the winter and in the summer, the same behaviour of the temperature in the catchment is observed until after 90 days, at which time the influence of the temperature of the injected water (5°C colder in winter and 5°C hotter in summer) starts to show.

Regarding the radii of thermal influence on the catchment level, in Fig.0-4 it can be seen how, at the end of the geothermal operation (after 150 days), the temperature varies 2.7°C and 1.6°C (winter and summer respectively) in the central area of the model (location of the probes). The radius of influence obtained in the catchment area is approximately 40 m for the winter and summer scenarios with $10 \text{ m}^3/\text{h}$ of flow rate.

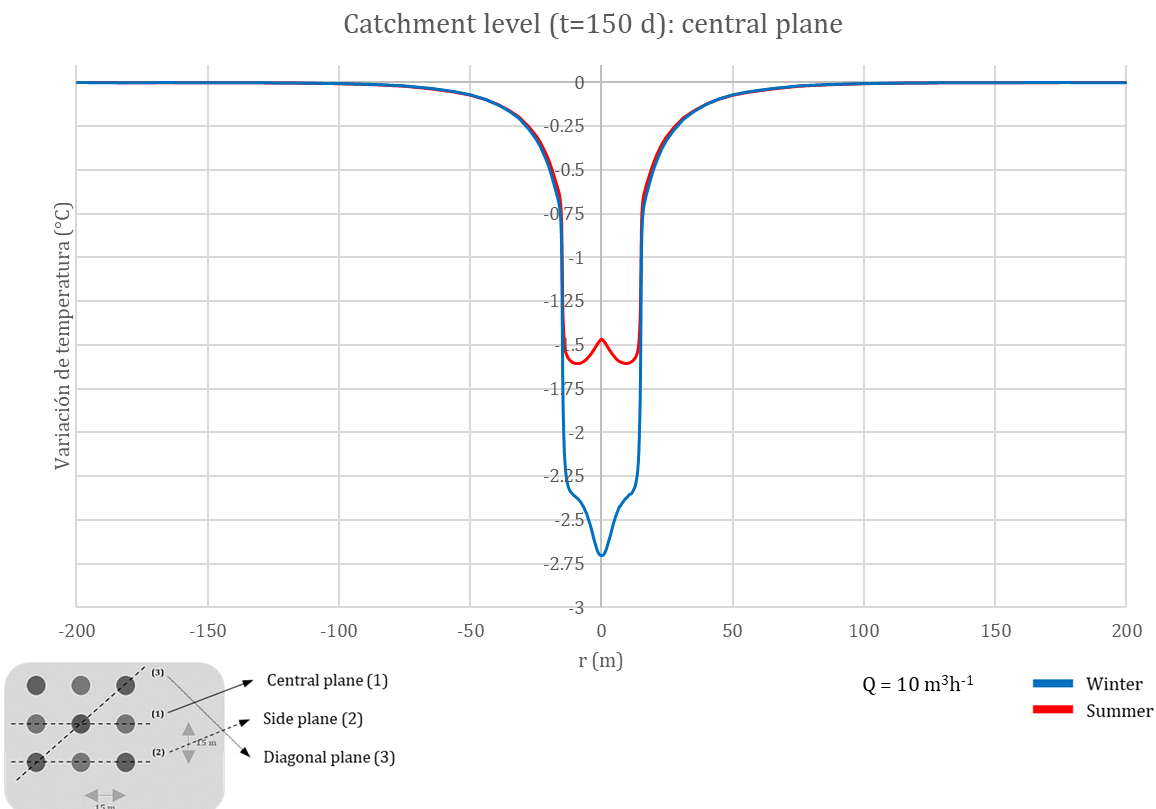


FIG. 0-4. Thermal influence at the catchment level in the proposed scenarios at the end of the geothermal operation ($t=150$ d) in the central evaluation plane.

Finally, Figs. 0-5 and 0-6 show the isotherms in the central evaluation plane resulting from the simulation of different scenarios (winter and summer seasons), with an operating flow rate of $10 \text{ m}^3/\text{h}$, at the end of the geothermal operation ($t=150\text{d}$).

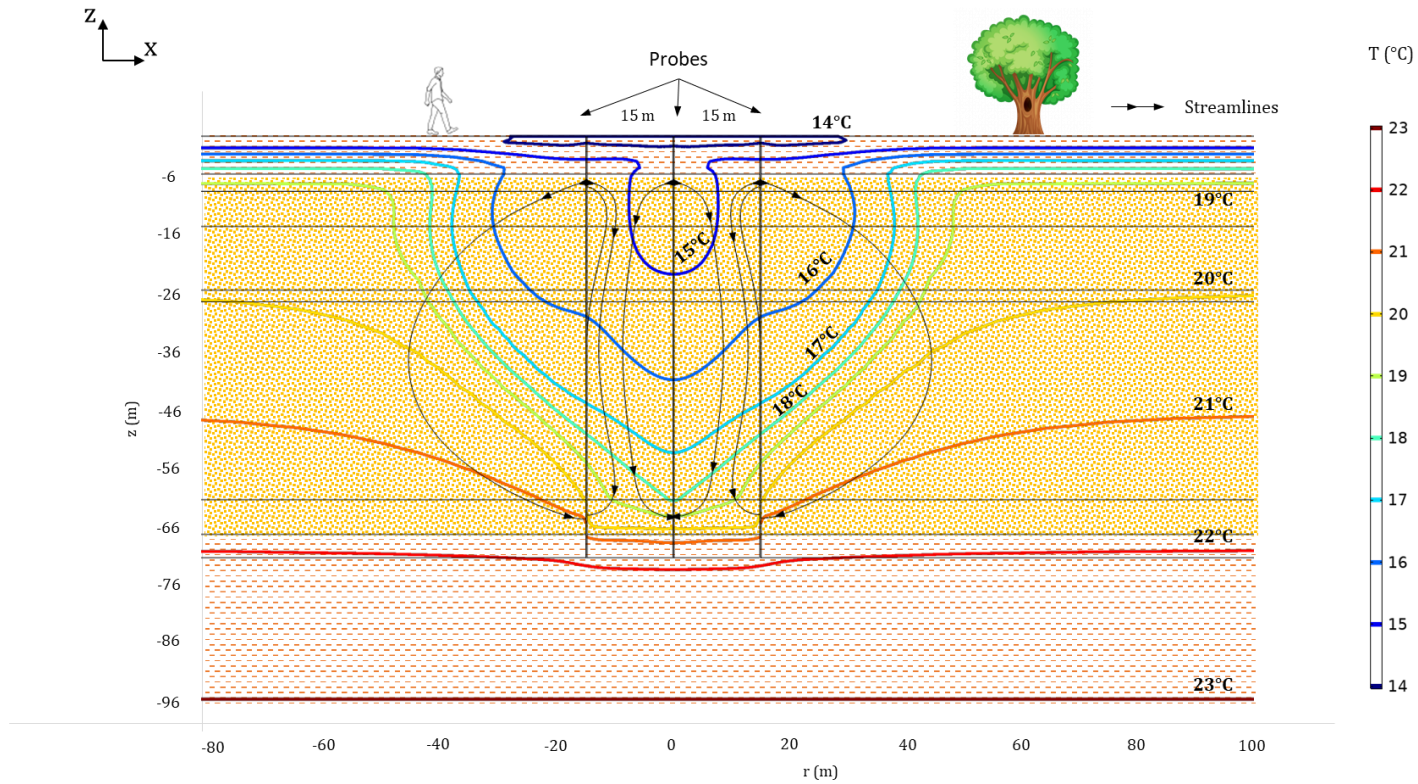


FIG. 0-5. Visualization example of the results obtained from the numerical simulation. Isotherms of the system (central evaluation plane) after 150 days of geothermal operation in the **winter season**, with an operating flow of $10 \text{ m}^3 \cdot \text{h}^{-1}$.

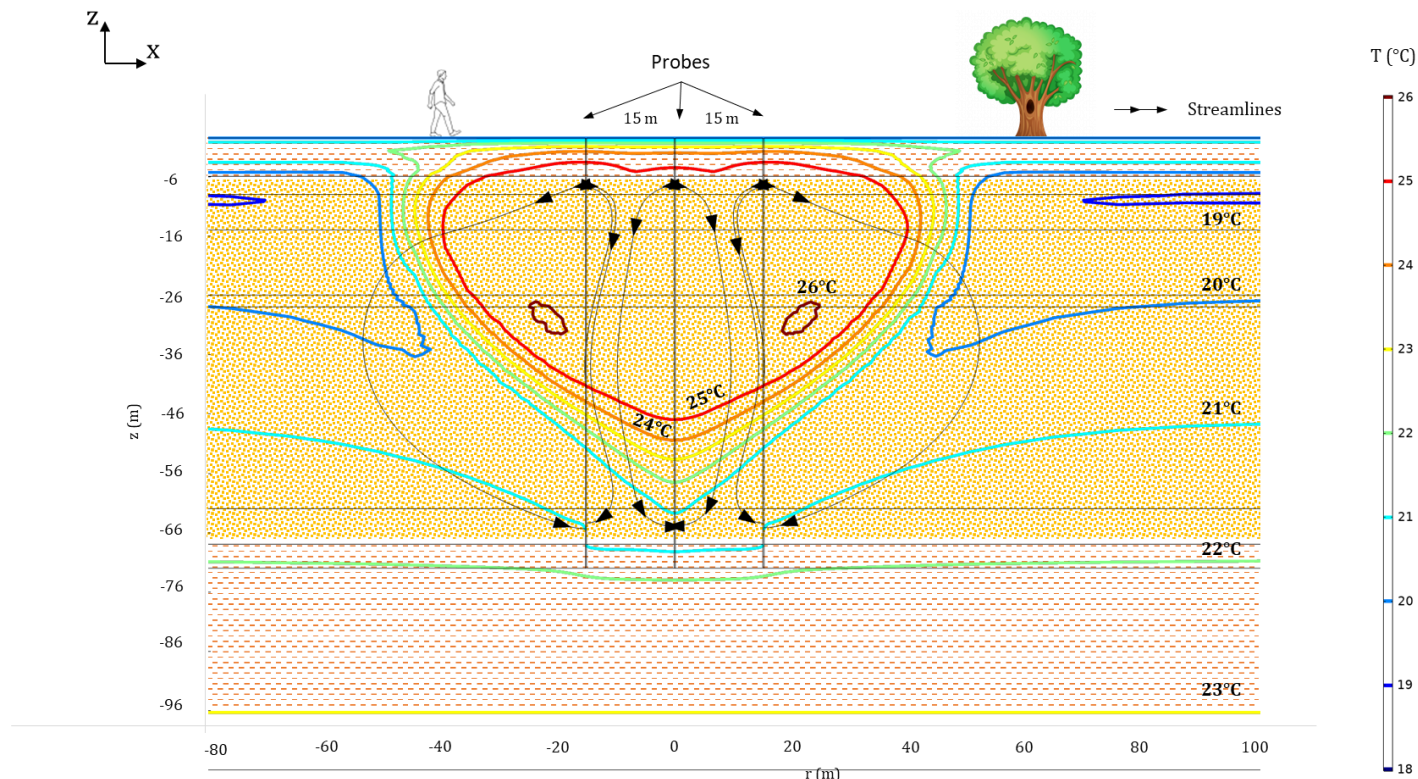


FIG. 0-6. Visualization example of the results obtained from the numerical simulation. Isotherms of the system (central evaluation plane) after 150 days of geothermal operation in the **summer season**, with an operating flow of $10 \text{ m}^3 \cdot \text{h}^{-1}$.



The main conclusion of this annex is that, for a system of probes such as the one presented here, the operation into an aquifer of high permeability is still possible at the cost of deepening the extraction point at depth.

The results presented here considered parameter values for a conservative estimate, that is: a **very high hydraulic conductivity** of ($10^{-3} \text{ m}\cdot\text{s}^{-1}$, see *sandy gravels* parameters considered in table 2) has been assigned to the aquifer as well as the highest operational flow.

The results show that under these conditions, doubling the separation between catchment and the reinjection points will keep the thermal impact at the catchment level on the aquifer under reasonable values.